Structural Evidence for Non-canonical Binding of Ca²⁺ to a Canonical EF-hand of a Conventional Myosin*⒮

Judit É. Debreczeni[‡1], **László Farkas**[§], **Veronika Harmat**[‡], **Csaba Hetényi**[§2], **István Hajdú**[¶], **Péter Závodszky**[¶],
Kazuhiro Kohama[‖], and **László Nyitray**[§3]

From the [§]*Department of Biochemistry, Eötvös Loránd University, Budapest H-1117, Hungary, the* [‡]*Protein Modeling Group,
Hungarian Academy of Sciences, Eötvös Loránd University, Budapest H-1117, Hungary, the* [‖]*Department of Pharmacology, Gunma
University, Maebashi 371-8510, Japan, and the* [¶]*Institute of Enzymology, Biological Research Center, Hungarian Academy of
Sciences, Budapest H-1117, Hungary*

We have previously identified a single inhibitory Ca²⁺-binding site in the first EF-hand of the essential light chain of *Physarum* conventional myosin (Farkas, L., Malnasi-Csizmadia, A., Nakamura, A., Kohama, K., and Nyitray, L. (2003) *J. Biol. Chem.* **278,** 27399–27405). As a general rule, conformation of the EF-hand-containing domains in the calmodulin family is "closed" in the absence and "open" in the presence of bound cations; a notable exception is the unusual Ca²⁺-bound closed domain in the essential light chain of the Ca²⁺-activated scallop muscle myosin. Here we have reported the 1.8 Å resolution structure of the regulatory domain (RD) of *Physarum* myosin II in which Ca²⁺ is bound to a canonical EF-hand that is also in a closed state. The 12th position of the EF-hand loop, which normally provides a bidentate ligand for Ca²⁺ in the open state, is too far in the structure to participate in coordination of the ion. The structure includes a second Ca²⁺ that only mediates crystal contacts. To reveal the mechanism behind the regulatory effect of Ca²⁺, we compared conformational flexibilities of the liganded and unliganded RD. Our working hypothesis, *i.e.* the modulatory effect of Ca²⁺ on conformational flexibility of RD, is in line with the observed suppression of hydrogen-deuterium exchange rate in the Ca²⁺-bound form, as well as with results of molecular dynamics calculations. Based on this evidence, we concluded that Ca²⁺-induced change in structural dynamics of RD is a major factor in Ca²⁺-mediated regulation of *Physarum* myosin II activity.

Conventional myosins (class II) have a fundamental role in muscle contraction and in a variety of cellular motilities. The globular heads of myosins consist of the motor domain responsible for the enzymatic activity and actin binding, and the so-called regulatory domain (RD),[4]

which acts as a lever arm during force generation, and it is the site of regulation in regulated conventional myosins. The essential and regulatory light chain subunits (ELC and RLC) bind to the lever arm to stabilize its structure. They belong to the EF-hand family of Ca²⁺-binding proteins, including calmodulin (CaM), the ubiquitous eukaryotic Ca²⁺ sensor; however, most of the divalent cation-binding sites of ELC and RLC have been lost during evolution. The two heads continue in a long coiled-coil dimer, which is responsible for filament formation under physiological conditions (for a review, see Ref. 1). Generally, the motor activity is switched on by an increase in intracellular Ca²⁺ concentration, either by direct binding to the ELC in molluscan myosins (2) or via the CaM-myosin light chain kinase system in smooth and nonmuscle myosins (3). Uniquely, a class II myosin of the slime mold *Physarum polycephalum*, generating the oscillatory cytoplasmic streaming in plasmodia, is inhibited by direct Ca²⁺ binding (4, 5). Ca²⁺ also has, however, more complicated regulatory effects on the function of many classes of unconventional myosins where the light chain subunits are CaM or CaM-like proteins (6–8).

Up to now, a detailed structural model of RD has been available only for the scallop muscle myosin (9, 10). Each light chain binds to an IQ motif (consensus sequence: IQ*XXX*RG*XXX*R) of the heavy chain (HC), stabilizing its α-helical structure. The N-terminal lobe of scallop ELC is in a "closed" state despite the fact that Ca²⁺ is bound to the first EF-hand. This EF-hand loop has an unusual, non-canonical sequence and unique Ca²⁺ coordination (10). The atomic model of the scallop RD and of the complete myosin head in different structural states (10–12) represents the "on" state of the myosin. The "off" state requires additional head-tail and head-head interactions (13) and has not yet been visualized at high resolution. Besides the scallop RD structure, two crystal structures and one homology model of CaM or CaM-like light chains bound to unconventional myosin IQ motifs have been described, but only in the apo-form (14–16).

We have previously provided evidence that the single inhibitory Ca²⁺-binding site of *Physarum* myosin is located in the first EF-hand of ELC, similar to the scallop myosin regulatory Ca²⁺ site (17). Mutational analysis of the EF-hand suggested that the Ca²⁺-saturated N-terminal lobe of ELC is in a closed state. In the present work, we have reported the structure of the Ca²⁺-bound *Physarum* RD at 1.8 Å resolution. The structure unambiguously showed that Ca²⁺ is indeed bound to a fully closed N-terminal lobe of ELC. Characterization of dynamic properties of both the apo- and the Ca²⁺-loaded RD by hydrogen-deuterium exchange experiments and molecular dynamics simulations enabled us to get a more detailed view of conformational fluctuations following Ca²⁺ binding. Based on the results, we have proposed a simple model to explain the modulatory effect of Ca²⁺ on the activity of *Physarum* myosin, in which Ca²⁺-induced alteration in the internal dynamics of RD

provides the basis for allosteric regulation. Preliminary results of this work have been presented elsewhere (18).

EXPERIMENTAL PROCEDURES

Protein Preparation—*Physarum* RD was prepared as described earlier (17). Briefly, the three-chain complex (ELC, RLC, and myosin HC fragment Ile-771–Gly-841) was expressed from a pET15b vector-based recombinant DNA in *Escherichia coli* BL21(DE3) cells and lysed under native condition by sonication. The cleared lysate was applied to a Ni^{2+}-affinity column followed by anion-exchange chromatography on a MonoQ column. Purity of the protein solution was examined on 15% SDS-PAGE. In some samples, the N-terminal His tag was removed by thrombin cleavage before the ion-exchange chromatography. The RD was extensively dialyzed against solution A containing 10 mM Tris-HCl, pH 7.6, 10 mM $CaCl_2$, 0.1 mM dithiothreitol and then concentrated to ~10 mg/ml by centrifugation with a Centricon filter unit (cut-off: 30 kDa).

Crystallization and Preparation of Heavy Atom Derivatives—Crystals were grown at 4 °C by vapor diffusion in hanging drops containing equal volume of protein in solution A and reservoir solution (20% polyethylene glycol 4000, 0.5 M NaAc, pH 4.6, 0.1 M NH_4Ac, 0.05 M NaCl). The crystals belong to the primitive orthorhombic space group $P2_12_12_1$ and have unit cell dimensions $a = 55.57$ Å, $b = 70.86$ Å, $c = 97.88$ Å, with one molecule in the asymmetric unit. After unsuccessful attempts of molecular replacement, heavy atom derivatives were prepared by soaking the crystals in 5–20 mM solutions of samarium, europium, holmium, ytterbium, mercury, and lead salts. Europium, lead, and mercury caused the crystals to crack, and the other derivatives were found to be isomorphous.

Data Collection and Structure Determination—Data sets were collected from single crystals at 100 K with a 165-mm-diameter MAR Research CCD detector at the ID 14-1 beamline at European Synchrotron Radiation Facility. As a cryo-protectant, 30% polyethylene glycol 400 was used. Images were processed with Denzo and Scalepack (19). ShelxD (20) was employed to find the heavy atom positions based on anomalous signals. Since the heavy atom sites had the same position in the different derivatives, only the ytterbium derivative, which afforded the highest resolution and the strongest anomalous signal, was used in further steps. Heavy atom sites were refined, and the first electron density map was calculated with Sharp (21) from isomorphous data combined with anomalous scattering. Phases were improved using the programs Solomon and dm (22, 23). Auto-building of the structure was tried with ArpWarp (24); subsequent runs built about 70% of the structure. For hand editing of the structure, the program XtalView (25) was employed; refinement was carried out with Refmac (26). Data statistics are listed in Supplemental Table One. It is notable that identical models were obtained from crystals that were grown from RD either with or without removal of the N-terminal His tag from the HC fragment.

Hydrogen/Deuterium Exchange—The kinetics of hydrogen-deuterium exchange in D_2O was measured by a Bruker IFS 28 Fourier-transformed infrared spectrophotometer. CaF_2 cells with a path length of 110 μm were used both for the sample and for background measurements. Measurements were carried out at 30.0 $\pm$ 0.1 °C, controlled with a Techne TU 16D temperature controller. The samples were dialyzed in 0.05 M MES, pH 6.0, and 2 mM $CaCl_2$ or in 2 mM EGTA, lyophilized above liquid nitrogen for 9 h, and then dissolved (1.5–2 mg of protein) in D_2O. The IR spectra (400–4000 cm^{-1} region) were recorded starting 30–50 s after complete dissolution. Absorbances of the amide I and amide II bands were evaluated from the spectra at the wave numbers of their maxima, *i.e.* at 1650 and 1547.5 cm^{-1}, respectively. The values
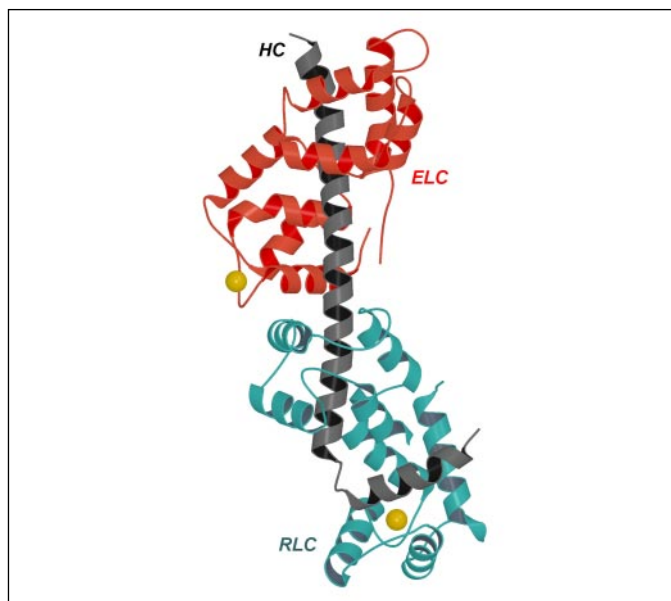

FIGURE 1. **Overall structure of *Physarum* myosin regulatory domain at 1.8 Å resolution.** A ribbon representation of the three-chain regulatory domain complex is shown. *Red*, essential light chain; *blue*, regulatory light chain; *gray*, heavy chain fragment (Ile-771–Gly-841). The inhibitory Ca^{2+} ion, bound to EF-hand I of ELC, and a crystal packing Ca^{2+} in EF-hand II of RLC (coordinated partially by a crystal symmetry-related ELC) are shown as *yellow spheres*. The figures were prepared by MolScript and Raster3D (62, 63).

were corrected with the baseline absorbances measured at 1789 cm^{-1}. The fraction of unexchanged hydrogens (X) was calculated from the ratio of amide II and amide I absorbances, taking the values of the unexchanged proteins and the completely deuterated ones as 100 and 0%, respectively. The results were presented as relaxation spectra (27), *i.e.* plotting X versus log (k_0t) as suggested by Závodszky *et al.* (28), where k_0 is the chemical exchange rate constant, which was calculated from the empirical expression, $k_0 = (10^{-pHread} + 10^{pHread-6})10^{0.05(T-25)}$ s^{-1}.

Molecular Dynamics Calculations—*Physarum* RD structure with two Ca^{2+} ions bound at the inhibitory and crystal packing binding sites, respectively, and the same structure without the Ca^{2+} ions were inputs of two separate MD calculations. The GROMACS (29) program package was used for the whole MD procedure, *i.e.* the preparation of the simulation box, the addition of water molecules for the explicit water model, energy minimizations, position-restrained preconditioning, and the 10-ns-long unrestrained MD runs at temperature of 300 K. The GROMOS (30) force field, particle-mesh Ewald method (31) for long range electrostatics, and LINCS (32) algorithm for bond constraints were utilized. The total charge was neutralized by the addition of counter ions. The r.m.s. deviation of substructures of *Physarum* RD, number of H-bonds, and interaction energy between the light chains were calculated with standard GROMACS analysis tools for the whole 10-ns trajectories. The protein structure at $T = 0$ ns was used as a reference of r.m.s. fit before r.m.s. deviation calculations.

RESULTS

Overall Description of the Structure—Fig. 1 shows the 1.8 Å resolution crystal structure of the *Physarum* myosin RD. It displays all the general features of the neck regions of a conventional myosin, as seen before in the crystal structures of scallop myosin RD and, in less detail, of chicken skeletal myosin subfragment 1 (33). The RD complex has an elongated shape; the two light chains stabilize the long α-helical segment of the heavy chain. There is a pronounced hook region in the HC near the C-terminal end, where the N-lobe of RLC binds to it. The C-terminal lobes of both *Physarum* light chains are in the same semi-
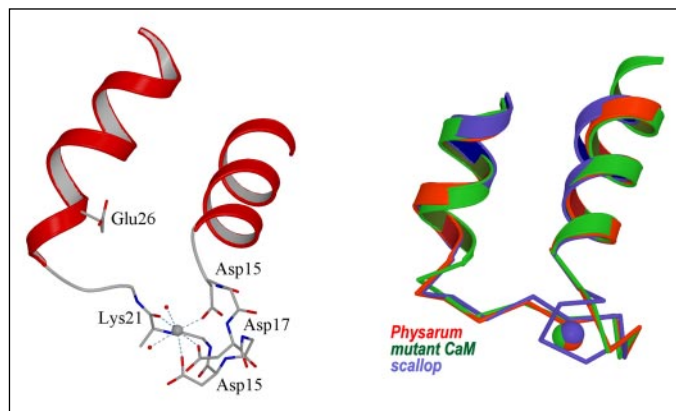
FIGURE 2. **Structure and comparison of the Ca²⁺ binding EF-hands of ELC and CaM.**
A, octahedral coordination of Ca²⁺ ion in the first EF-hand of ELC showing an unusual closed conformation. Ca²⁺ is coordinated by Asp-15, Asp-17, Asp-19, Lys-21, and two water molecules (*red dots*). Glu-26, which normally provides a bidentate ligand for Ca²⁺ in the open state, is too far in the structure to participate in coordination of the ion. *B*, comparison of the Ca²⁺ binding EF-hand I of the *Physarum* (*red*) and scallop myosins (*blue*; Protein Data Bank accession code 1wdc) and the mutant CaM structure (*green*; 1y6w) reveals high similarity between the *Physarum* and the mutant CaM structure. Note the extra turn in the first helix of scallop ELC. r.m.s. deviations of the backbone carbons, after superimposing the scallop and calmodulin structures, are 0.53 Å.

open conformation as in the scallop RD (10) and also in an apo-CaM/two IQ complexes and the CaM-like Mlc1p/IQ complexes of class V myosin (15, 16). The semi-open conformation provides strong binding of the LCs/CaMs to the first part of an IQ motif. The N-terminal lobe of ELC displays a closed conformation despite the fact that the first EF-hand, which has been shown to be the inhibitory Ca²⁺-binding site of *Physarum* myosin (17), contains a bound Ca²⁺ ion. This domain, like that of the scallop RD, binds to the second part of the first IQ motif with rather external surface contacts. There is only a slight bend in the HC helix, where it interacts with the N-lobe of ELC. The structure of both the N-terminal and the C-terminal lobes shows high similarity to the corresponding lobes of scallop RD, with r.m.s. deviations for backbone superimpositions of 0.81 and 1.18 Å, respectively. The two lobes of RLC when compared with the corresponding lobes of scallop myosin gave similar r.m.s. deviation values (1.53 and 1.14 Å). However, the above comparisons also highlight variability of the orientations that the two lobes can adopt on different myosins. For instance, the N- and C-lobes of RLC are in closer proximity in the *Physarum* RD; therefore, the inter-lobe interactions more extensively stabilize the sharp bending of the HC. The flexible nature of the interlobe linkers could also have functional implications as it was pointed out by comparing RDs of scallop myosin head crystal structures in different functional states (12). The N-terminal domain of RLC, in good accordance with the scallop structure, forms an open structure and interacts strongly with hydrophobic residues of the "hook" region of the HC, although its first EF-hand cannot bind divalent cations (17). Unexpectedly, a second Ca²⁺ ion was located in the electron density, bound to the second EF-hand of RLC, which mediates crystal contacts. We will argue that this site has no biological importance and that its occupation by Ca²⁺ does not significantly affect our structural and functional interpretations.

Inhibitory Ca²⁺-binding Site in the First EF-hand of ELC—The striking feature of the crystal structure is that the Ca²⁺-bound N-terminal lobe adopts a closed conformation, whereas in the case of other conventional EF-hand proteins, the lobe conformation is generally open when a divalent cation is bound. As shown in Fig. 2*A*, four amino acid residues and two water molecules are involved in the formation of an octahedral coordination geometry; Asp-15, Asp-17, Asp-19 are liganded to the Ca²⁺ ion by one of their carboxyl oxygens, and Lys-21 is coordinated by

its carbonyl oxygen. All coordinating residues are homologous with the liganding residues in CaM, and they are also in the same conformation. However, in the *Physarum* ELC, in contrast to CaM, residues after the eight position of the Ca²⁺-binding loop cannot be involved in the coordination since the domain is in a closed conformation. The second (exiting) helix of this EF-hand displaced, and the residues after the ninth position are removed from the vicinity of the Ca²⁺ ion. To stabilize the binding of the ion, Glu-26 at the 12th position of the loop is substituted by a water molecule. The sixth ligand is a second water molecule, similarly to the canonical binding structure (34, 35). Since Glu-26 would act as a bidentate ligand but was replaced by a water molecule, the Ca²⁺ site has six ligands instead of the usual seven. The loop may accommodate cations of similar size due to the fact that one of the water molecules, completing the coordination sphere, is not supported by any residues directly; therefore, its position may be slightly adjusted to meet the need of the cation. This would account for the observed Mg²⁺ binding of this site (17).

The unusual closed state is stabilized, and the closed-to-open conformational transition is prevented by several factors. First of all, the second EF-hand, which cannot bind any cation, can stabilize the closed state of the whole N-terminal lobe through cooperative interactions. Stability of the closed state is also provided by the short antiparallel β-sheet segments at the end of the loops. Moreover, specific interactions between the HC and the first two helices of ELC fix the relative position of the N-terminal lobe adequately for a closed lobe conformation. The corresponding lobe of the scallop ELC is also in a closed state; however, it was argued that this Ca²⁺-binding site is in an EF-hand with non-canonical liganding residues, and the site is stabilized only by extensive interactions with RLC and the HC helix (10). Comparison of the Ca²⁺-binding EF-hands of *Physarum* and scallop ELC (Fig. 2*B*) shows that the first helix of scallop ELC has an extra turn allowing the unique binding of Ca²⁺ in the closed state with additional stabilizing interactions with the RLC. EF-hand I of the *Physarum* structure lacks this extra helical turn and in fact has a fully canonical loop structure. Finally, lack of methionine residues in the N-lobe of *Physarum* ELC (and only one in scallop ELC) could also be a structural factor preventing the large conformational transition; it was suggested that methionine side chains may facilitate Ca²⁺-induced opening in EF-hands of the CaM superfamily (36). Interestingly, the structure of the Ca²⁺-saturated N-lobe of *Physarum* ELC is very similar to the recently reported crystal structure of a mutant Ca²⁺-bound CaM locked in the closed conformation by a disulfide bond (Fig. 2*B*) (37). r.m.s. deviations of the backbone carbons after superimposing EF-hand I and EF-hand II of the N-lobes are 0.53 and 0.80 Å, respectively. The author has reasoned that the structure represents the transition state of the Ca²⁺ switch (37). Apparently, the Ca²⁺-induced close-to-open transition in the N-lobe of ELC also has a high activation barrier imposed on the structure by the interactions described above, and the lobe conformation freezes in a sort of transition state of the close-to-open isomerization.

N-terminal Lobe of RLC—The whole N-lobe of RLC adopts an open conformation, although EF-hand I does not bind a cation. As described above, the lobe conformation can be stabilized by various forces, such as HC-LC interactions and cooperative bonds between the two EF-hand regions, and not solely by the binding of a divalent cation. In the case of scallop myosin RLC, although the second loop cannot bind a metal ion, the presence of Mg²⁺ in the first loop, together with the binding of the HC target helix, results in the conformational transition to the open form of the whole domain. The open state is apparently the consequence of the binding mode of the domain to the hook region of the HC, which is similar to other amphipathic CaM target sites (38, 39) and does
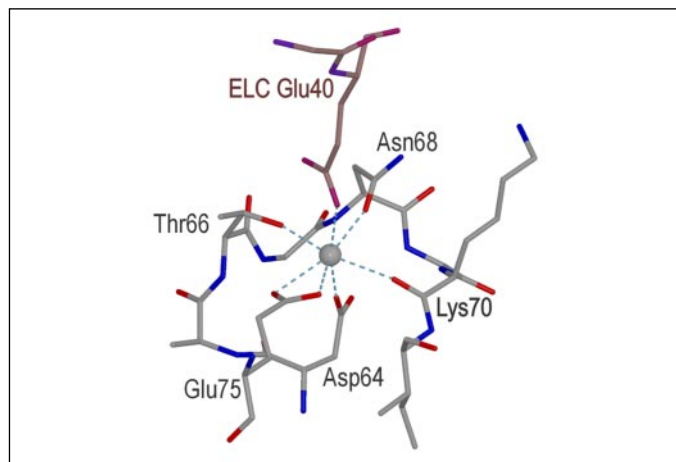
FIGURE 3. **Ca²⁺ coordination in the second EF-hand of the RLC.** The coordination sphere of this Ca²⁺ ion differs from that of the canonical Ca²⁺ binding of calmodulin-like proteins as the seventh ligand is provided by Glu-40 of a symmetry mate of ELC (carbon atoms in *brown*). The Ca²⁺ ion and carbon atoms of the RLC are colored *gray*. N and O atoms are shown in *atomic colors*. Note that this site has no physiological relevance.

not necessarily require binding of divalent ions to its first EF-hand. This seems to be a general feature of RLCs in lower eukaryotes, which are unable to bind any divalent metals.

The asymmetric unit of the crystal structure contains a second bound Ca²⁺ in the second EF-hand of the RLC, coordinated by seven oxygen atoms arranged similarly to other, canonical EF-hands. As shown in Fig. 3, five residues are involved in the binding: Asp-64, Asn-68, and Thr-66 by their side chain oxygens, Lys-70 by its carbonyl oxygen, and Glu-75 by both of its side chain oxygens as a bidentate ligand. The seventh ligand is provided by Glu-49 of a crystal symmetry-related ELC, instead of a water molecule as found in other EF-hand proteins. The rather uncommon way of Ca²⁺ coordination raises the question whether this Ca²⁺-binding site has any physiological function. No biochemical data exist that would indicate binding of Ca²⁺ or Mg²⁺ to *Physarum* myosin II in solution beyond the well characterized Ca²⁺-binding site of ELC (4, 5, 17). Moreover, aside from the liganding residue from ELC, only a single H-bridge can be seen between the RLC and the symmetry-related ELC, which cannot be regarded as a specific bond between the two molecules. Therefore, we have suggested that the second Ca²⁺ mediates only packing interactions during crystallization and that this site is unlikely to contribute to the open state of the lobe. However, one cannot rule out that the actual lobe orientation and the angle at the HC hook are slightly affected by the unusual ligand-mediated crystal contact.

Bends in the Heavy Chain Helix—The interface between the two LCs is not as extended as observed in the scallop RD. These interactions are not sufficient to position the two chains in a relatively fixed position like the numerous H-bonds and van der Waals contacts at the ELC-RLC interface in scallop RD, suggesting that the Ca²⁺ binding does not require an extensive cooperative interaction network. As a probable consequence of the fewer interchain linkages, the HC is bent only slightly (~10°) between the two IQ motifs when compared with ~40° in the scallop RD and the chicken skeletal S1 structures (Fig. 4).

At a sharp bend of the HC (the hook at the RLC interlobe region), the angle is almost 135° in *Physarum* RD structure, whereas it is only ~90° in the scallop and skeletal RD structures (Fig. 4). Moreover, the RD leans in the opposite directions in the *Physarum* RD. The beginning of the HC helix, the so-called pliant region at the motor domain/lever arm junction of the myosin head (12), is straight in the *Physarum* RD structure as in the scallop S1 and not bent as in the smooth muscle crystal structure (40). The same salt bridge stabilizes the pliant region as in the scallop
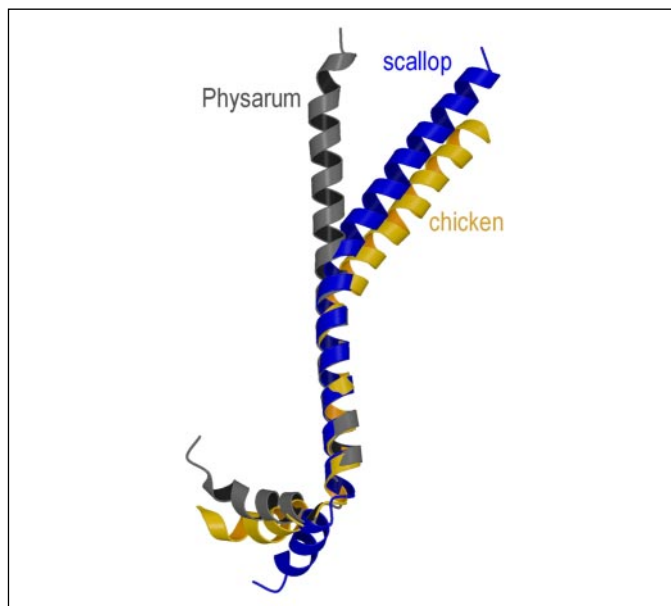

FIGURE 4. **Conformation of the heavy chain in the *Physarum*, scallop muscle and chicken skeletal muscle myosin RD, respectively.** A least squares superposition of the long helical neck region from the *Physarum* (*gray*), scallop (*blue*; Protein Data Bank accession code 1wdc), and chicken (*yellow*; 2mys) myosins is shown. The *Physarum* RD shows the sharpest bend at the hook region (RLC interlobe interface) and the smallest bend at the ELC-RLC interface.
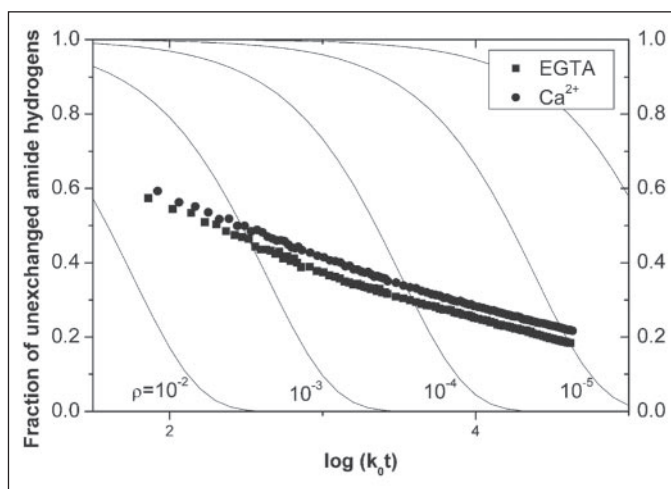

FIGURE 5. **Hydrogen-deuterium exchange of RD in the presence and absence of Ca²⁺ ions.** The hydrogen-deuterium exchange data, summarized in the form of relaxation spectra for *Physarum* myosin II at 25 °C, pD 6.55, are shown. The fraction of unexchanged hydrogens was calculated from the ratio of amide II (1547.5 cm⁻¹) and amide I (1650 cm⁻¹) absorbances, taking the values of the unexchanged proteins and the completely deuterated ones as 100 and 0%, respectively. The chemical exchange rate constant, k_0, was calculated by the equation $k_0 = (10^{-pHread} + 10^{pHread-6})10^{0.05(T-25)}$ s⁻¹ where *T* is time (see "Experimental Procedures"). The *solid lines* represent the exchange rate curves for hypothetical polypeptides characterized by a given probability (the ρ values) of solvent exposure of the peptide groups. The curves indicate higher conformational flexibility for the Ca²⁺-free (*square*) when compared with the Ca²⁺-bound (*circle*) RD.

structure. The above facts indicate that the position of the myosin heads and the initial part of coiled-coil rod could be quite different in the myosin isoforms.

Hydrogen-Deuterium Exchange Experiments—Our efforts to obtain suitable crystals for structure determination in the absence of Ca²⁺ ions failed. Either crystals did not grow or preformed crystals were shattered if they were treated with EGTA. To obtain additional information of the Ca²⁺-free RD structure, we performed hydrogen-deuterium exchange

experiments. Recording and analysis of the time course of hydrogen-deuterium exchange followed by Fourier-transformed infrared spectroscopy is a powerful tool to compare conformational flexibilities and micro-stabilities of protein molecules. The regulation of myosin involves conformational rearrangements of the structure, which is likely to be accompanied by alterations of internal mobility. These alterations are presumably transient considering scallop myosin RD (10, 12), but no prior result was known about the regulation of *Physarum* myosin. As shown in Fig. 5, the internal mobility of *Physarum* RD both in the presence and in the absence of Ca^{2+} was relatively high. In the Ca^{2+}-free sample, the average probability of solvent exposure of buried hydrogens is 2-fold higher than in the Ca^{2+}-saturated one, concerning the whole pattern of the hydrogen-deuterium exchange experiment. The observed shift in the relaxation spectra can be explained if one assumes that binding of Ca^{2+} increases the overall conformational stability of the RD by suppressing conformational fluctuations. The parallel position of the two relaxation spectra means that the accessibility of virtually all detectable peptide hydrogens increases in the Ca^{2+}-free form of RD. These results denote a moderately, but significantly higher, global flexibility within the RD in the absence of Ca^{2+}, and moreover, they suggest that the increased rigidity of the RD could contribute to inhibition of the motor activity upon Ca^{2+} binding to *Physarum* myosin.

Molecular Dynamics Calculations—To learn more of the dynamic behavior of the *Physarum* RD in the presence and absence of Ca^{2+}, we performed *in silico* molecular dynamics calculations. During a 10-ns simulation time, the Ca^{2+} ion remained bound at the inhibitory binding site, whereas the other Ca^{2+} ion at the crystal packing site dissociated from the RD at ~3 ns, further indicating that it is a weakly bound, physiologically non-important Ca^{2+}, which is present only in the crystals. The r.m.s. deviation plot of the Ca^{2+}-free structure of *Physarum* RD shows significantly higher (2–4 Å) fluctuations when compared with that of the Ca^{2+}-saturated complex (1–2 Å; Fig. 6*A*). It should be remarked that r.m.s. deviation plots of substructures of the RD show similar, or in some cases, even higher degree of fluctuations (data available upon request). Comparison of interaction energies revealed that the interaction between the two LCs in the Ca^{2+}-loaded RD is significantly stronger than without bound Ca^{2+} during the MD trajectory (Fig. 6*B*). This energy difference can be assigned partly to the difference in the number of H-bonds between the interacting loops of ELC and RLC as shown in Fig. 6*C*. Although most regions of the complex in the Ca^{2+}-free state show higher mobility, interestingly, in the hook and the C-terminal region of the HC helix, the structural fluctuations show an opposite tendency, *i.e.* they show higher rigidity in absence of Ca^{2+}. This fact might be related to our inference that the bound Ca^{2+} in RLC is only a crystal artifact and could even slightly destabilize the RLC-HC interactions. The molecular dynamics calculations confirm our hydrogen-deuterium exchange experiments that Ca^{2+} binding to the RD decreases the global internal mobility of the complex.

DISCUSSION

Ca^{2+}-binding Sites of Physarum Conventional Myosin—We have previously identified and characterized a single inhibitory Ca^{2+}-binding site in the first EF-hand of the CaM-like ELC of *Physarum* myosin. Mutagenesis studies suggested that the bound Ca^{2+} does not induce the close-to-open transition of the N-terminal lobe of ELC (17) as usually, although not exclusively, found in the CaM family of EF-hand proteins (41, 42). Although a notable exception of the above rule is the non-canonical closed N-lobe of ELC in the scallop myosin (10), it was argued that the closed Ca^{2+}-bound state in that system is likely the consequence of the unusual sequence and coordination of the EF-hand. Here
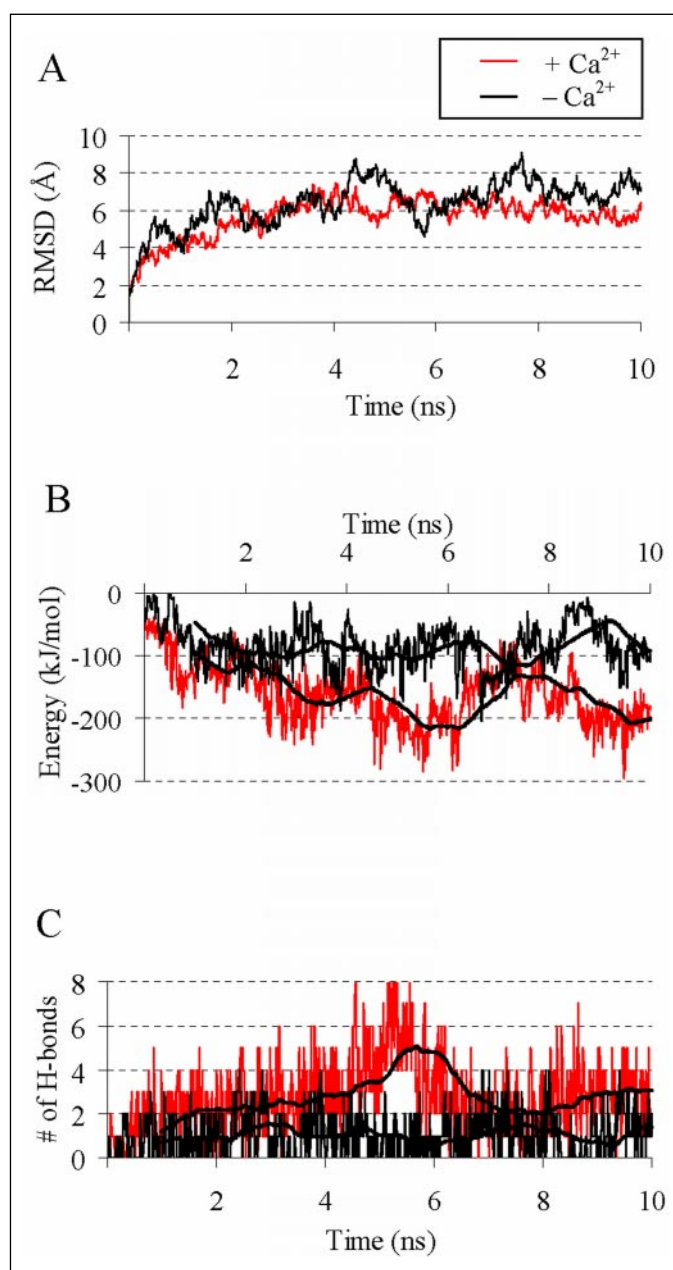

FIGURE 6. **Molecular dynamics simulation of *Physarum* myosin RD.** The analysis of trajectories of the 10-ns-long molecular dynamics simulations on Ca^{2+}-bound (*red*) and Ca^{2+}-free (*black*) *Physarum* RD structures is shown. The GROMACS program package (31) was used for the whole MD procedure. *A*, r.m.s. deviation fluctuation of all atoms shows remarkably larger flexibility if the two Ca^{2+} ions are removed from the structure. Intermolecular interaction energy (*B*) is lower and the number of corresponding H-bonds (*C*) is higher between ELC and RLC in the case of Ca^{2+}-bound *Physarum* RD. For the latter two diagrams, moving averages are shown as *black lines* for ease of comparison.

we have provided evidence that even a canonical EF-hand of a myosin ELC is able to bind Ca^{2+} without the large conformational change. The structure shows that Ca^{2+} is bound to a fully closed N-terminal lobe of ELC. The second part of the binding loop is not involved in Ca^{2+} coordination, and the position of the exiting helix does not need to open relative to the entering helix upon Ca^{2+} binding; therefore, the closed conformation of the lobe does not conflict with cation binding. Our results strongly suggested that the closed state of the N-lobe of a Ca^{2+}-saturated ELC is a general feature of all class II myosins that are able to bind Ca^{2+}, regardless of the functional effect of the bound cation: acti-

vation in molluscan muscle myosin, inhibition on *Physarum* plasmodial myosin, and no known effect on *Dictyostelium* myosin.

The presence of the crystal packing Ca^{2+} site in the *Physarum* RD structure raises concerns whether the bends in the HC helix and the lobe orientation of the RLC are affected by the crystal contact artifact. We strongly believe that it is not the case. Weak binding of the crystal contact Ca^{2+} to the N-lobe of RLC, as demonstrated by MD simulations, could induce only slight changes. Moreover, even a high affinity Ca^{2+} does not induce pronounced rearrangement of the LC lobes or the HC bends, as found in the recently obtained Ca^{2+}-free structure of scallop RD; instead of large-scale structural changes, the apo structure shows higher structural mobility,[5] in line with our findings. Finally, it is important to note that crystal contact-mediating intermolecular Ca^{2+} ions, without affecting the structure of the EF-hand proteins, were also observed in oncomodulin and CaM crystals, respectively (43, 44).

Ca^{2+} Inhibition of Physarum Myosin and Its Comparison with Ca^{2+} Activation of Scallop Myosin—Our working hypothesis is that Ca^{2+} binding induces only a small-scale conformational change in the RD and that decrease in the motor activity of *Physarum* myosin II is rather caused by alteration in the internal dynamics of the protein. Hydrogen-deuterium exchange results and molecular dynamics simulations supported this view and showed that the most obvious difference between the Ca^{2+}-loaded RD and the apoRD is an increase in the rigidity of the liganded structure. Based on these results, we have proposed a simple model to explain the inhibitory effect of Ca^{2+}. In the Ca^{2+}-free state, higher conformational flexibility of the RD is required for the proper functioning of the lever arm and full activity of the motor. Binding of Ca^{2+} to the N-lobe of ELC alters the dynamics of the RD. A slight increase in rigidity could alter the orientation of the lever arm relative to the motor and the tail domains (in Fig. 4, note the unusual orientation of the hook helix, which would position the head relative to the tail in an orientation that could not easily interact with actin) and/or impose some strain on the RD and consequently could prevent full force generation. Diminished ATPase activity of the myosin motor may slow down cytoplasmic streaming in the plasmodium and allow turning over the direction of streaming caused by Ca^{2+} oscillation, which is regulated by a so far unknown mechanism (45).

The effects of Ca^{2+} on the local conformation of ELC and on the dynamics of RD seem to be similar in *Physarum* and scallop myosin II; Ca^{2+} dissociation from ELC results in only minor changes in the crystal structure of scallop RD but increases internal mobility.[5] Increased internal mobility of the Ca^{2+}-free scallop RD was also observed by fluorescence and ESR spectroscopy (46).[6] However, the Ca^{2+} switch is more complicated in scallop myosin; the heads are in a unique off conformation in the absence of Ca^{2+}. Removal of Ca^{2+} increases mobility of the RD only transiently (10), allowing the two heads as well as the two RDs and the tail to interact and assume an asymmetric off-state conformation (13, 47, 48), similar to the dephosphorylated off-state of smooth muscle myosin (49). Binding of Ca^{2+} to the RD increases rigidity that would impose strains on the asymmetric head-head and head-tail interactions, freeing the heads and thus switching the motor on. Direct communication between the RD and the motor domain has been demonstrated by extensive kinetic studies of scallop heavy meromyosin (47); therefore, any change in the flexibility of the RD could indeed influence the motor activity.

The Ca^{2+} inhibition/activation difference between the two conventional myosins must be due to differences in the consequence of

dynamic changes on the whole myosin (like the off state of scallop myosin) and to additional structural differences, such as bends in the HC and/or interactions of the RD with the motor domain, which may transmit the Ca^{2+} signal in opposite manners to the active site. Full understanding of the opposite regulatory effect of Ca^{2+}-binding on scallop and *Physarum* myosin clearly necessitates further structural studies of myosin fragments with full activity. Alterations in conformational dynamics as a structural basis of Ca^{2+} regulation in conventional myosin are not unique among Ca^{2+}-binding proteins; it was proposed that various activities of CaM in response to Ca^{2+} may primarily result from changes in the dynamic properties of its structure (44).

Implications for Ca^{2+} Regulation of CaM-binding Unconventional Myosins—Our structure could provide some insight into the Ca^{2+} binding and regulation of unconventional myosins that have CaM or CaM-like light chain subunits bound to IQ motifs of the HC. Based on sequence comparisons (17), *Physarum* ELC (and all known ELCs from lower eukaryotes) shows higher similarity to mammalian CaM than to its ELC orthologs (~43 and ~35% identity with mammalian CaMs and ELCs, respectively). Ca^{2+} binding to CaM has a complicated effect on the activity of unconventional myosins (6–8, 50–52) that may require different degrees of saturation of CaM with Ca^{2+} and also different regulatory mechanisms. For instance, it was proposed that Ca^{2+}-induced dissociation from, and bridging of, IQ motifs in myosin-V could regulate its function (16, 53). It is reasonable to assume that dissociation of CaM from the IQ sequence must be preceded or accompanied by a closed-to-open transition of at least one of its domain. However, if the IQ-bound CaM is only partially saturated with Ca^{2+}, it is possible that there is only a subtle change of its conformation. CaM in the apo form was shown to bind to its respective IQ motifs as binding of the ELC to the IQ motifs of conventional myosins, *i.e.* the N-lobe only loosely attaches to the side of the HC, whereas the C-lobe assumes the characteristic grabbing semi-open conformation (14, 15). Based on the structure of *Physarum* RD, containing a CaM-like ELC, we hypothesized that Ca^{2+} could also bind to the IQ-bound CaM without inducing the closed-to-open transition of the N-terminal lobe but still having regulatory role. This could be one of the mechanisms by which Ca^{2+} binding releases the inhibition of the motor imposed by tail domain in myosin V (54–56). We predicted that the *Physarum* ELC structure represents a partially saturated Ca^{2+}-bound conformation of CaM when it binds to an IQ motif. The C-terminal lobe of ELC is in a semi-open state, which is important for the strong binding to the first part of the IQ motif, and this conformation rules out the possibility of metal binding; if Ca^{2+} binds to this lobe, it must trigger CaM dissociation from the IQ motif, as observed in myosin-I (7). In the N-terminal lobe of CaM, Ca^{2+} could bind in the closed conformation without much steric constrain. In case the Ca^{2+} concentration is further increased and both EF-hands are saturated, cooperative transitions would lead to the opening of the sites and the consequent dissociation of CaM as found in class I and V myosins (57, 58). An alternative scenario could be if Ca^{2+} binding only releases the N-lobe that binds to an adjacent empty IQ site, forming a bridging complex of the lever arm, as proposed to occur in myosin-V (16, 53).

Conclusion—The crystal structure of the RD of *Physarum* myosin II revealed a Ca^{2+}-bound EF-hand in a closed lobe conformation. Our results suggested that ELCs of all Ca^{2+} binding conventional myosins are Ca^{2+} sensors without undergoing a large conformational transition of the binding site to regulate their motor activity, whereas CaMs bound to IQ motifs function either with a large structural switch or with a more subtle conformational change. Hydrogen-deuterium exchange experiments and molecular dynamics calculations highlight the importance of changes in conformational flexibility to explain the molecular basis of

---

allosteric regulation in both conventional and perhaps unconventional myosins, similar to the regulation of many other proteins (59–61).

REFERENCES

1. Sellers, J. R.(1999) *Myosins*, Oxford University Press, Oxford **2,** 1323–1423
2. Szent-Gyorgyi, A. G., Kalabokis, V. N., and Perreault-Micale, C. L. (1999) *Mol. Cell Biochem.* **190,** 55– 62
3. Trybus (1991) *Cell Motil. Cytoskeleton* **18,** 81– 85
4. Kohama, K., and Kendrick-Jones, J. (1986) *J. Biochem.* (*Tokyo*) **99,** 1433–1446
5. Kohama, K., Kohno, T., Okagaki, T., and Shimmen, T. (1991) *J. Biochem.* (*Tokyo*) **110,** 508–513
6. Wolenski, J. S. (1995) *Trends Cell Biol.* **5,** 310–316
7. Zhu, T., Beckingham, K., and Ikebe, M. (1998) *J. Biol. Chem.* **273,** 20481–20486
8. Yokota, E., Muto, S., and Shimmen, T. (1999) *Plant Physiol.* **119,** 231–240
9. Xie, X., Harrison, D. H., Schlichting, I., Sweet, R. M., Kalabokis, V. N., Szent-Gyorgyi, A. G., and Cohen, C. (1994) *Nature* **368,** 306–312
10. Houdusse, A., and Cohen, C. (1996) *Structure* (*Lond.*) **4,** 21–32
11. Houdusse, A., Szent-Gyorgyi, A. G., and Cohen, C. (2000) *Proc. Natl. Acad. Sci. U. S. A.* **97,** 11238 –11243
12. Gourinath, S., Himmel, D. M., Brown, J. H., Reshetnikova, L., Szent-Gyorgyi, A. G., and Cohen, C. (2003) *Structure* (*Camb.*) **11,** 621–1627
13. Stafford, W. F., Jacobsen, M. P., Woodhead. J., Craig, R., O'Neall-Hennessey, E., and Szent-Gyorgyi, A. G. (2001) *J. Mol. Biol.* **307,** 137–147
14. Houdusse, A., Silver, M., and Cohen, C. (1996) *Structure* (*Lond.*) **4,** 1475–1490
15. Houdusse, A., Trybus, K., and Cohen, C. (2000) *Biophys. J.* **78,** 158a
16. Terrak, M., Wu, G., Stafford, W. F., Lu, R. C., and Dominguez, R. (2003) *EMBO J.* **22,** 362–371
17. Farkas, L., Malnasi-Csizmadia, A., Nakamura, A., Kohama, K., and Nyitray, L. (2003) *J. Biol. Chem.* **278,** 27399 –27405
18. Farkas, L., Debreczeni, J., Harmat, V., Kohama, K., Nakamura, A., and Nyitray, L. (2001) *J. Muscle Res. Cell Motil.* **22,** 591a
19. Otwinowsky, Z., and Minor, W. (1997) *Methods Enzymol.* **276,** 307–326
20. Sheldrick, G. M., Hauptmann, H. A., Weeks, C. M., Miller, M., and Usón, I. (2001). *Ab initio phasing. International Tables for Crystallography*, (Arnold, E., and Rossmann, M., eds) Vol. F, pp 333–351, Kluwer Academic Publishers, Dordrecht, The Netherlands
21. Fortelle, E. de la, and Bricogne, G. (1997) *Methods Enzymol.* **276,** 472– 494
22. Abrahams, J. P., and Leslie, A. G. W. (1996) *Acta Crystallogr. Sect. D Biol. Crystallogr.* **52,** 30 – 42
23. Cowtan, K. (1994) *Joint CCP4 and ESF-EACBN Newsletter on Protein Crystallography*, Number 31, pp. 34 –38, Daresbury Laboratory, Warrington, UK
24. Perrakis, A., Morris, R. J., and Lamzin, V. S. (1999) *Nat. Struct. Biol.* **6,** 458 – 463
25. McRee, D. E. (1999) *J. Struct. Biol.* **125,** 156 –165
26. Murshudov, G. N., Vagin, A. A., and Dodson, E. J. (1997) *Acta Crystallogr. Sect. D Biol. Crystallogr.* **53,** 240 –255
27. Závodszky, P., Johansen, J. T., and Hvidt, A. (1975) *Eur. J. Biochem.* **56,** 67–72
28. Závodszky, P., Kardos, J., Svingor, A, and Petsko, G. A. (1998) *Proc. Natl. Acad. Sci. U. S. A.* **95,** 7406 –7411
29. Lindahl, E., Hess, B., and van der Spoel, D. (2001) *J. Mol. Mod.* **7,** 306 –317
30. van Gunsteren, W. F., Billeter, S. R., Eising, A. A., Hünenberger, P. H., Krüger, P., Mark, A. E., Scott, W. R. P., and Tironi, I. G. (1996) *Biomolecular Simulation: The GROMOS96 Manual and User Guide*, Hochschulverlag AG an der ETH, Zurich
31. Darden, T., York, D., and Pedersen, L. (1993) *J. Chem. Phys.* **98,** 10089 –10092
32. Hess, B., Bekker, H., Berendsen, H. J. C., and Fraaije, J. G. E. M. (1997) *J. Comp. Chem.* **18,** 1463 –1472
33. Rayment, I., Rypniewski, W. R., Schmidt-Base, K., Smith, R., Tomchick, D. R., Benning, M. M., Winkelmann D. A., Wesenberg, G., and Holden, H. M. (1993) *Science* **261,** 50 –58
34. Babu, Y. S., Sack, J. S., Greenhough, T. J., Bugg, C. E., Means, A. R., and Cook, W. J. (1985) *Nature* **315,** 37– 40
35. Babu, Y. S., Bugg, C. E., and Cook, W. J. (1988) *J. Mol. Biol.* **204,** 191–204
36. Nelson, M. R., Chazin, W. J. (1998) *Protein Sci.* **7,** 270 –282
37. Grabarek, Z. (2005) *J. Mol. Biol.* **346,** 1351–1366
38. Meador, W. E., Means, A. R., and Quiocho, F. A., (1992) *Science* **257,** 1251–1255
39. Meador, W. E., Means, A. R., and Quiocho, F. A. (1993) *Science* **262,** 1718 –1721
40. Dominguez, R., Freyzon, Y., Trybus, K. M., and Cohen, C. (1998) *Cell* **94,** 559 –571
41. Yap, K. L., Ames, J. B., Swindells, M. B., and Ikura, M. (1999) *Proteins* **37,** 499 –507
42. Vetter, S. W., and Leclerc, E. (2003) *Eur. J. Biochem.* **270,** 404 – 414
43. Ahmed, F. R., Rose, D. R., Evans, S. V., Pippy, M. E., and To, R. (1993) *J. Mol. Biol.* **230,** 1216 –1224
44. Wilson, M. A., and Brunger A. T. (2000) *J. Mol. Biol.* **301,** 1237–1256
45. Nakamura A., and Kohama K. (1999) *Int. Rev. Cytol.* **191,** 53–98
46. Malnasi-Csizmadia, A., Hegyi, G., Tolgyesi, F., Szent-Gyorgyi, A. G., and Nyitray, L. (1999) *Eur. J. Biochem.* **261,** 452– 458
47. Nyitrai, M., Szent-Gyorgyi, A. G., and Geeves, M. A. (2003) *Biochem. J.* **370,** 839 – 848
48. Wendt, T., Taylor, D., Trybus, K. M., and Taylor, K. (2001) *Proc. Natl. Acad. Sci. U. S. A.* **98,** 4361– 4366
49. Jung, H. S., Burgess, S. A., Colegrave, M., Patel, H., Chantler, P. D., Chalovich, J. M., Trinick, J., Knight, J. (2004) *Biophys. J.* **86,** 403a
50. Trybus, K. M., Krementsova, E., and Freyzon, Y. (1999) *J. Biol. Chem.* **275,** 27448 –27456
51. Yoshimura, M., Homma, K., Saito, J., Inoue, A., Ikebe, R., and Ikebe, M. (2001) *J. Biol. Chem.* **276,** 39600 –39607
52. Homma, K., Saito, J., Ikebe, R., and Ikebe, M. (2001) *J. Biol. Chem.* **276,** 34348 –34354
53. Martin, S. R., and Bayley, P. M. (2004) *Protein Sci.* **11,** 2909 –2923
54. Wang, F., Thirumurugan, K., Stafford, W. F., Hammer, J. A., 3rd, Knight, P. J., and Sellers, J. R. (2004) *J. Biol. Chem.* **279,** 2333–2336
55. Krementsov, D. N., Krementsova, E. B., and Trybus, K. M. (2004) *J. Cell Biol.* **164,** 877– 886
56. Li, X. D., Mabuchi, K., Ikebe, R., and Ikebe, M. (2004) *Biochem. Biophys. Res. Commun.* **315,** 538 –545
57. Homma, K., Saito, J., Ikebe, R., and Ikebe, M. (2000) *J. Biol. Chem.* **275,** 34766 –34771
58. Martin, S. R., and Bayley, P. M. (2004) *FEBS Lett.* **567,** 166 –170
59. Mazon H., Marcillat O., Forest E., and Vial C. (2004) *Protein Sci.* **13,** 476 – 486
60. Shen T., Tai K., Henchman R. H., and McCammon J. A. (2002) *Acc. Chem. Res.* **35,** 332–340
61. Berendsen H. J., and Hayward S. (2000) *Curr. Opin. Struct. Biol.* **10,** 165–169
62. Kraulis, P. J. (1991) *J. Appl. Crystallogr.* **24,** 946 –950
63. Merritt, E. A., and Bacon, D. J. (1997) *Methods Enzymol.* **277,** 505 –524